

Chapter 5

Discussion

In this chapter we consider the results obtained from isotopic studies of CAIs from the Efremovka and Grosnaja meteorites along with other available data from these CAIs to understand the processes leading to their formation, as well as time scales for certain early solar system processes and solar-stellar relationship. The primary emphasis during isotopic analyses of CAIs was to look for possible departures in the measured isotopic ratios from the normal solar system (reference) values. Such departures, if present, can serve as extremely useful tracers to probe the above aspects.

The discussion presented in this chapter is divided into five subsections.

- (i) Processes affecting the formation of CAIs,
- (ii) Relict spinels and nebular environment for the formation of CAIs,
- (iii) Mg-Al isotopic systematics and isotopic heterogeneity in the nebula,
- (iv) ^{41}Ca in the early solar system,
- (v) Extinct radionuclides and time scales for early solar system processes.

5.1 Processes Affecting the Formation of CAIs

Studies of isotope mass fractionation in CAIs allows one to delineate the nature of their source material and the principle processes leading to their formation. For example, positive mass fractionation in magnesium isotopes [$F(\text{Mg}) > 0$] would imply evaporative residue as the source material for CAIs as such residues are expected to be enriched in heavy isotopes. Conversely, mass fractionation favouring the lighter isotopes [$F(\text{Mg}) < 0$] in CAI would suggest their formation by condensation from a gas depleted in heavy isotopes.

Both melilite and spinel phases in the Efremovka coarse-grained CAIs analyzed in this work are generally enriched in their heavy isotopes i.e. $F(\text{Mg}) > 0$ (see Tables 4.1-4.4; Fig. 5.1). Even though there is an apparent trend for a higher $F(\text{Mg})$ value for spinel compared to melilite (e.g. E65, E44), we do not consider this difference to be significant in view of the measurement uncertainties in $F(\text{Mg})$ [typically $\sim 1.5\%/amu$ ($2\sigma_m$)]. Positive mass fractionation is clearly evident in five (E36, E44, E50, E59, E65) of the CAIs analyzed. In the case of E2 and E40, $F(\text{Mg})$ values for melilite and spinel show certain systematic spatial variation. In E2 a few data points for rim spinel and near-rim phases do show $F(\text{Mg}) \leq 0$, however, the $F(\text{Mg})$ values for melilite in the inclusion interior are positive. In the case of E40, the interior melilites have near normal or slightly above normal Mg isotopic composition, but the values are much higher for melilites and spinels near the rim as well as many spinel grains in the interior. The $F(\text{Mg})$ values in the multizoned hibonite-rich inclusion E50 show non-systematic spatial variations, but both melilite and spinel are generally enriched in the heavier isotopes: the $F(\text{Mg})$ values in the melilite-perovskite zone are near normal, in the melilite-spinel zone both melilite and spinel have high $F(\text{Mg})$ values, and in the inclusion interior, melilite in both the hibonite-rich zone and in areas where it is in association with perovskite have $F(\text{Mg}) \geq 0$. Although the values for the type B2 inclusion E60 are near normal, there is a hint in the data for a positive $F(\text{Mg})$ value. The general trend for positive $F(\text{Mg})$ values for the Efremovka coarse-grained CAIs suggest evaporative residue as the source material for these objects. This is in accord with what one generally expects for coarse-grained refractory inclusions based on earlier work on CAIs

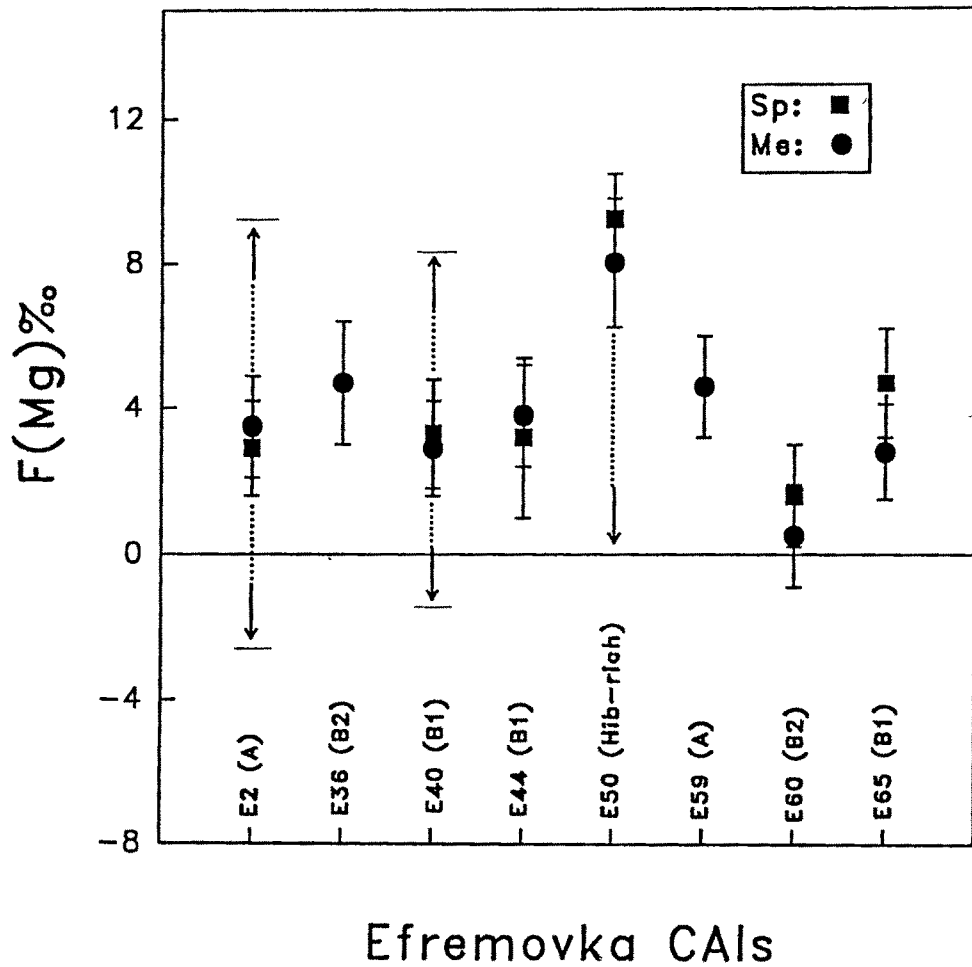


Figure 5.1: The intrinsic mass fractionation $F(\text{Mg})$ in the melilite (Me) and spinel (Sp) phases of the Efremovka CAIs analyzed in this study are shown. In the case of E2, E40, and E50 the range of $F(\text{Mg})$ values is indicated by the arrow marks. Note that within experimental uncertainty melilite and spinel have similar $F(\text{Mg})$ values. In the case of E36 and E59 $F(\text{Mg})$ values were measured only for melilite.

from other meteorites (Esat and Taylor, 1984; Clayton et al., 1988; MacPherson et al., 1988). There is no hint in the data for extreme magnesium isotope mass fractionation, and none of the Efremovka inclusions studied in this work can be classified as so called FUN inclusion, characterized by high $F(\text{Mg})$ values, typically $>10\%$ (Wasserburg et al. 1977, Brigham 1990).

The results obtained for the spatial variation in $F(\text{Mg})$ in the Efremovka CAIs (Tables 4.1 and 4.4) suggest a significant and systematic difference in $F(\text{Mg})$ values between peripheral and interior phases only in E2 and E40.

The spatial variation in $F(\text{Mg})$ for these two CAIs [E2 and E40] showed extremely contrasting trends (Figs. 5.2-5.3). Such trends could result from either isotopic exchange between distinct reservoirs or specific process(es) affecting these inclusions during their formation and evolution. The $F(\text{Mg})$ trend seen by us in E2, where $F(\text{Mg})$ value increases from the near rim region to the inclusion interior agree with the results reported previously by Fahey et al. (1987b). The observed variation cannot be produced by an external thermal event affecting this inclusion during its formation. Fahey et al. (1987b) suggested that the $F(\text{Mg})$ trend seen in E2 can be approximated by a diffusion profile although the exact nature of the process leading to the observed trend cannot be determined. Diffusional exchange of magnesium between an isotopically normal and an isotopically heavy reservoir, the latter representing the parent material of E2, could be one of the possible mechanisms that can be proposed to explain the fractionation trend seen in this inclusion.

In contrast to E2, the fractionation trend in E40 (Fig. 5.3), with higher $F(\text{Mg})$ values for melilite near the inclusion boundary compared to that in the inclusion interior, is unique in the sense that this trend is seen for the first time in a normal (non-FUN) refractory inclusion. Before attempting to explain this trend in terms of physical processes affecting this inclusion, we note that the melilite near the rim of E40 is gehlenitic (high Al/Mg ; more refractory) and it is akermanitic (low Al/Mg ; less refractory) in the interior (Fig. 5.3). We now consider several plausible scenarios that can explain either or both the isotopic and petrographic data. These include:

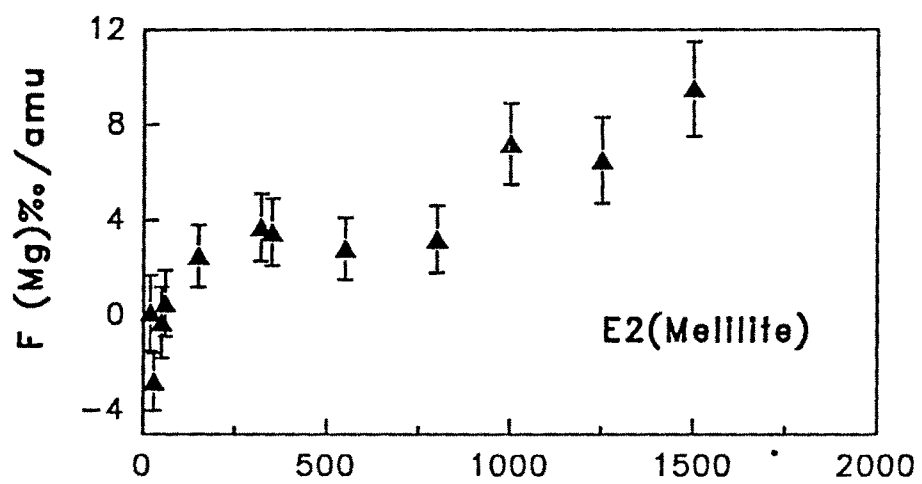


Figure 5.2: Magnesium isotopic mass fractionation in melilite from compact type A Efremovka CAI E2. F(Mg) values have been plotted as function of distance from the inner edge of the rim.

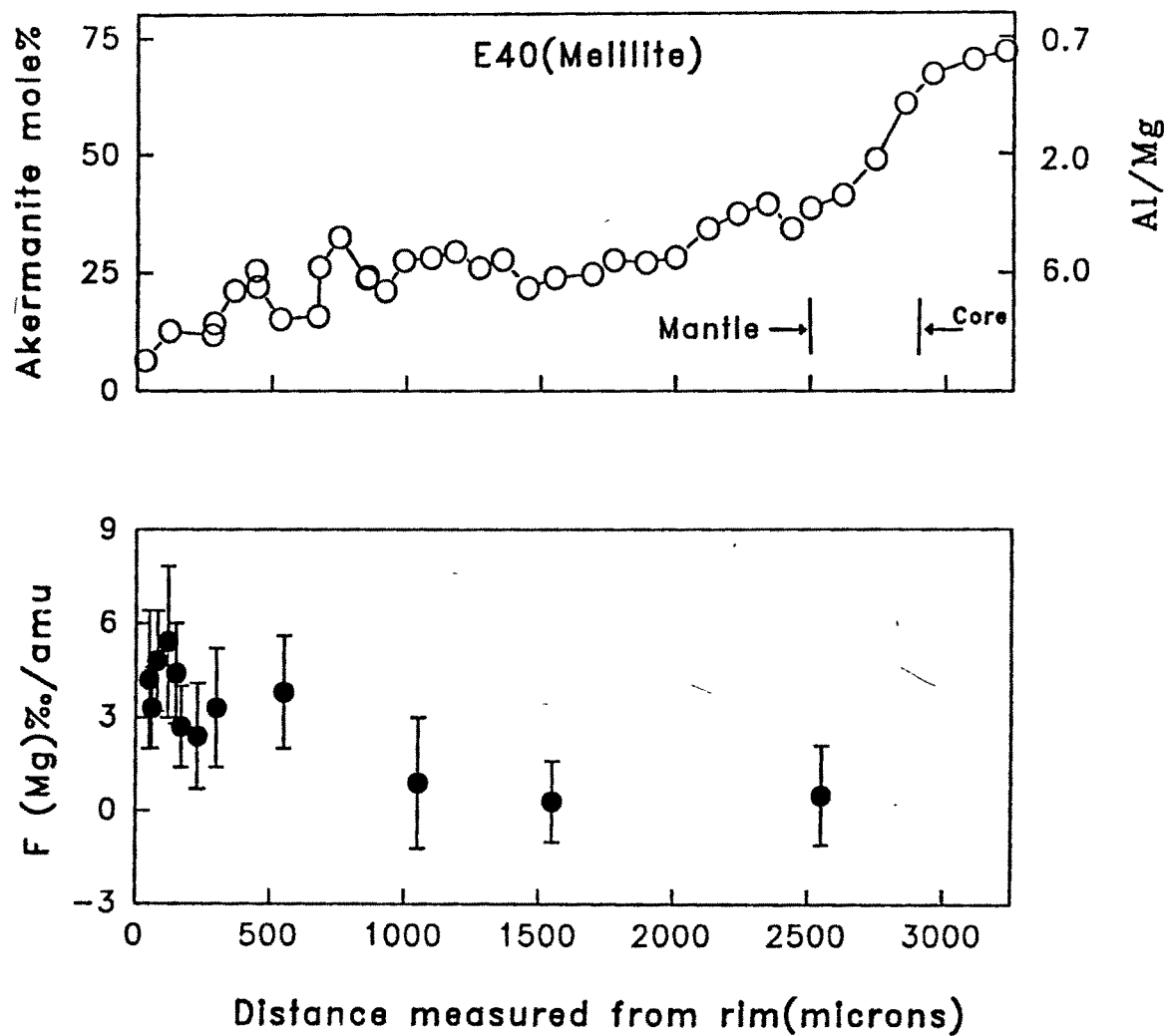


Figure 5.3: Electron probe data for akermanite content in melilite along a nearly radial traverse in type B1 Efremovka CAI E40. Ion microprobe data for magnesium isotopic mass fractionation in melilite close to this traverse is also shown. The akermanite content and $F(Mg)$ values show an inverse correlation. The approximate extent of the mantle melilite and the beginning of the core region are indicated.

- (i) isotopic exchange between parent melt of E40 and an external reservoir of appropriate composition,
- (ii) evaporation of Mg from E40 following its crystallization,
- (iii) evaporation of Mg from the parent melt of E40 prior to its crystallization.

If the trend is due to isotopic exchange, we need a positively fractionated external reservoir with $F(\text{Mg}) \geq 4\text{-}6\text{‰/amu}$ exchanging magnesium isotopes with a reservoir of normal isotopic composition, representing the parent material of E40. Even though a positively fractionated external magnesium isotopic reservoir is a difficult proposition, we cannot completely rule out such a scenario. Alternatively, one can also postulate that E40 evolved from a melt characterized by high $F(\text{Mg})$ that reequilibrated with an isotopically normal reservoir following the crystallization of melilite and spinel near the inclusion boundary. However, such a scenario appears ad-hoc as melilite crystallization in CAIs is a very quick processes (Wark and Lovering 1982, Stolper and Paque 1986), and there may not be enough time for reequilibration following the crystallization of melilite near the boundary, and prior to crystallization of melilite in the interior.

If the observed fractionation trend in E40 is due to a thermal event, e.g. processes (ii) or (iii) above, we need a heating episode during the formation of this inclusion that resulted in loss of magnesium from its boundary region. The most obvious process that could be responsible for this is a volatilization event affecting this inclusion. Since the petrographic features of E40, (the rounded shape, coarse grained texture and mineralogy) suggest its formation via melt crystallization, the volatilization event could have affected either the parent melt of E40 or the inclusion proper following its crystallization. However, experimental studies have shown that evaporation from solid can lead to positive mass fractionation in Mg isotopes only within the first few tens of micron of the surface (Wang et al. 1991). The observed fractionation effect in E40 (high $F(\text{Mg})$ values), on the other hand, persists up to a few hundred microns from the inclusion boundary. Therefore, evaporation from solid as a cause for the observed fractionation trend in E40 may be ruled out.

Finally, if we consider evaporation from the parent melt of E40, the observed increase in F(Mg) values near the surface as well as the lower akermanitic content (Δk_{10-15}) in this region, can be explained by considering a loss of $\leq 25\%$ Mg from a melt with a composition similar to the mantle region of E40 [$\Delta k_{25-35}\%$]. This follows from the experimental data obtained by Davis et al. (1990) who have measured the magnitude of isotopic fractionation in O, Mg and Si during evaporation of a melt of forsteritic composition. We would like to note that fractional crystallization from the parent melt of E40 could have led to the observed range of melilite composition in this inclusion. Therefore, it is *a priori* not necessary to invoke volatilization loss to explain the variation in the melilite composition near the boundary region of this inclusion. However, it is interesting to note that the proposed volatilization event with a loss of $\leq 25\%$ Mg from the boundary region can in fact lead to the progressive decrease of the Akermanitic content in the near rim region (Fig. 5.3) if the initial composition was similar to that of the mantle ($\Delta k_{25-30}\%$). The volatilization event leading to the observed magnesium isotope mass fractionation trend in E40 should also result in correlated oxygen and silicon isotope mass fractionations (Davis et al. 1990). The expected O and Si isotope mass fractionations are $\leq 4\%$ /amu and $\leq 2.5\%$ /amu respectively. Unfortunately, there are experimental difficulties in the measurement of oxygen isotopic ratios of insulating solids by the ion microprobe, and high instrumental mass fractionation for silicon in melilite ($\sim 50\%$ /amu) does not allow for a precise determination of the variation of F(Si) in E40 melilite. The absence of Ca-aluminate in E40, which is expected during intense evaporation of melilite [Δk_{50}] (Hashimoto, 1991), qualitatively suggests that the degree of evaporation in E40 was not extremely intense. There are however other Efremovka CAIs (e.g., E66a) where an association of gehlenite, perovskite, and Ca-aluminates is seen in their boundary regions. This perhaps resulted from a more intense evaporation process than in the case of E40. Since the proposed volatilization event affecting the parent melt of E40 can explain both the isotopic and compositional variation in melilite, we consider this to be a more plausible process compared to the isotopic exchange scenarios discussed earlier.

It is difficult to establish whether the proposed volatilization event was itself responsible for the formation of E40 or whether it was a secondary event that affected the parent

melt of E40 produced in a separate thermal event. However, the duration of the volatilization event has to be necessarily short so that the compositional gradient generated by it is not obliterated by melt diffusion. Clayton et al. (1984) and Davis et al. (1991) have proposed similar scenarios for explaining the nearly sympathetic petrographic and isotopic data for two forsterite-bearing FUN inclusions. *Although possible correlation between isotopic and petrographic data in CAIs have been conjectured before this is the first instance in which sympathetic behaviour has been seen in a normal (non-FUN) refractory inclusion.* This observation substantiates the role of volatilization and melt crystallization as important CAI forming processes.

5.2 Relict Spinel and Nebular Environment for the Formation of CAIs

The CAI E40 has texture and mineralogy that suggests its crystallization from a melt and the two dominant mineral phases in this inclusion, melilite and spinel, are expected to be in isotopic equilibrium. The spinels in this inclusion show some groupings in size; the spinels near the boundary are generally small (10-20 μm) compared to those in the inclusion interior (\sim 20-60 μm), and some spinels in the pyroxene rich core are close to 100 μm in size (Fig. 5.4). The F(Mg) values for different spinel groups provided a surprise. We found that the spatial variation in F(Mg) for spinel is not exactly similar to melilite. This can be seen in Fig. 5.5 where we show the data for magnesium isotope mass fractionation in both melilite and spinel across a couple of nearly radial traverses in this inclusion. The F(Mg) values for spinels near the boundary are generally high and similar to the melilite values, whereas the spinels in the inclusion interior show a spread in their F(Mg) values in contrast to melilite, whose F(Mg) values suggest near normal magnesium isotopic composition. The basic results that are evident in the data shown in Fig. 5.5 are:

- (i) small and medium sized spinels near the inclusion periphery have high F(Mg) that are similar and at times higher than melilite,



Figure 5.4: Photomicrographs of spinels from the boundary and interior regions of E40 showing clear size groupings. Scale bars are 20 and 100 μm respectively.

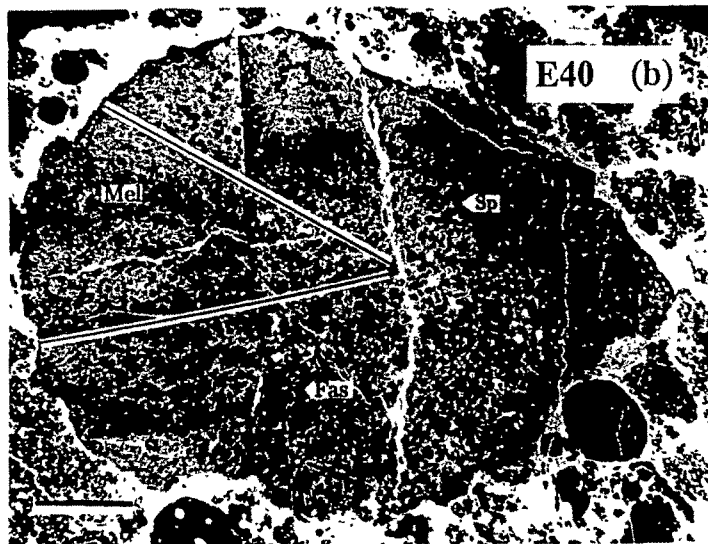
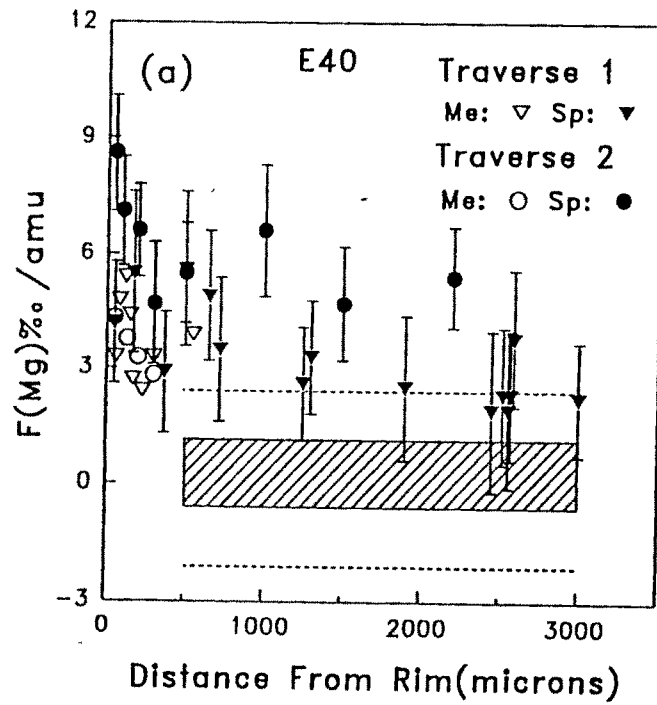


Figure 5.5: Magnesium isotopic mass fractionation in melilite and spinel (Fig.a) from Efremovka CAI E40 measured along two radial traverses (Fig.b). The measured range of melilite fractionation for the interior melilite ($\geq 500\mu\text{m}$) falls within the shaded area and the dotted line encompasses the extreme error limits of individual measurements in melilite.

- (ii) medium sized spinels in the inclusion interior have both low and high F(Mg) values; the lower F(Mg) values match those of melilite in the interior,
- (iii) large spinels in the core region have F(Mg) values similar to melilite in the interior.

The spinels with low F(Mg) in the inclusion interior may be considered to be in isotopic equilibrium with the melilite. However, the presence of spinels with F(Mg) values much greater than that for melilite in the inclusion interior was unexpected. One can consider two possible explanations for this observation:

- (i) movement of spinels with high F(Mg) values, initially present near the peripheral (near rim) region, into the inclusion interior during the crystallization of this CAI.
- (ii) the spinel grains with high F(Mg) are relict or extraneous to the inclusion.

We shall now consider these two possibilities. Laboratory based simulation experiments on the formation of CAIs similar to E40 (i.e. Type B1) were carried out by Wark and Lovering (1982). These experiments have led to the idea of movement of spinels from the periphery into the interior during crystallization of CAI resulting in spinel rich core, that are commonly observed in type B1 CAIs. In this scenario small spinel grains crystallize near the inclusion boundary about 20°C prior to melilite crystallization. However, once melilite starts crystallizing, they grow rapidly and push some of the spinel grains into the interior. These spinel grains continue to grow in the interior of the CAI and get trapped in late crystallizing phases. Since both melilite and spinel near the boundary of the inclusion E40 have high F(Mg), due to the volatilization event experienced by the parent melt of this CAI (Sec. 5.1), the presence of spinels with high F(Mg) values in the interior may be due to movement of boundary spinels as proposed by Wark and Lovering (1982). However, if this was the case, the small boundary spinels that were pushed into the interior would grow as they moved inward. Therefore, one would expect the spinel grains in the interior to have a core with high F(Mg) and a peripheral region with lower value of F(Mg) similar to that for melilite in the interior. However, we could not find such a difference in the F(Mg) values

for the edge and center of spinel grains in the interior, and such differences, if present, are definitely smaller than our measurement uncertainties ($\pm 1.5\text{‰}$ /amu). Therefore the spinel redistribution hypothesis can be ruled out as an explanation for the discordance in the isotopic data between melilite and spinel.

The other possibility that can readily explain the discordant $F(\text{Mg})$ data for spinel and melilite in E40 is that the spinels with distinctly different and high $F(\text{Mg})$ values compared to the melilite are extraneous to this inclusion and represent relict spinels. These spinels were present in the parent melt of E40 and retained their identity due to incomplete melting and lack of isotopic equilibration. We believe that some of the small and medium-sized spinels in the interior of E40 with $F(\text{Mg})$ values outside the melilite envelope are relict. Some of the small spinels near the boundary (e.g. first spinel data point) may also represent relict phases. It is difficult to make any specific comment about the relative abundance of relict spinels because of their random occurrence and possible sampling bias. While a good fraction of the small spinels could be relict, the fraction is much smaller for the medium sized spinels and none of the core spinels analyzed can be termed as relict. The relict spinels could have been present in the parent material of E40 or they were incorporated into the parent melt of E40 prior to its crystallization. In both the scenarios spinel grains can escape complete melting if the melt was spinel saturated (Ulyanov, 1991). The possible presence of relict phases in coarse-grained CAIs was suggested by Stolper (1982) and Stolper and Paque (1986) on the basis of results obtained from laboratory experiments aimed at understanding the crystallization sequence in these objects. Attempts to identify relict grains from studies of trace elements in coexisting mineral phases in CAIs have met only with limited success (e.g., Kuehner et al., 1989; Simon et al., 1991). Isotopic data, that are suggestive of the presence of relict phases in early solar system objects, are also rare and there are only a couple of observations that include those of Zinner et al. (1991), who argued for an extraneous origin of a magnesiowustite-metal fremdling in a CAI from Vigarano, and of Sheng et al. (1991a) who identified relict spinels in plagioclase-olivine-inclusions (POIs) from several carbonaceous chondrites. This study provides the first evidence for the presence of relict grain representing a major constituent phase of CAI. The implications

of the observation for the thermal evolutionary history of E40 in particular and CAIs in general are discussed below.

The observed isotopic disequilibrium between spinel and melilite in E40 suggest lack of isotopic exchange between the relict spinels and the parent melt of E40. This allows us to place limits on the cooling rate during crystallization of E40 if we have the following inputs:

- (i) Magnesium self diffusion constant in spinel in contact with Mg rich melt at high temperature,
- (ii) Initial temperature of the parent melt of type B1 CAIs to which E40 belongs.

Laboratory based simulation experiments have been conducted by Sheng et al. (1991b) to determine the Mg self diffusion constant in solid spinel in contact with a melt of composition similar to plagioclase-olivine inclusions. They observed that the self diffusion constant varies as a function of temperature and can be approximated by the Arrhenius Relation :

$$D = D_0 \exp(-E/RT) \quad (5.1)$$

where D is the diffusion constant, D_0 is the pre-exponential factor, R is the gas constant, T is the temperature and E is the activation energy. The values of D_0 for spinel and melt obtained by Sheng et al. (1991b) are 74.6 cm^2 and 7791 cm^2 respectively, while the activation energies (E) are $\sim 384 \text{ kJ}$ and $\sim 343 \text{ kJ}$ respectively. The initial melt temperature for type B1 CAI like E40 is expected to be between 1400°C to 1500°C . These values were inferred by Stolper and Paque (1986) who carried out simulation experiments designed to reproduce petrographic features of Type B inclusions starting with a melt of $\text{CaO-Al}_2\text{O}_3\text{-MgO-SiO}_2$ in appropriate proportions.

Based on these two sets of inputs viz. self diffusion constant of Mg in spinel and initial temperature of the parent melt of CAI like E40, one can obtain a relation between cooling

rate and spinel size demanding complete isotopic homogenization of the spinel with the melt. This relation given by Kaiser and Wasserburg (1983) can be written as:

$$(d/2)^2 = \frac{RT_o^2 D(T_o)}{r_o E} \quad (5.2)$$

where d is the minimum grain size (diameter) of spinel that will undergo isotopic homogenization with the melt, R is the gas constant, T_o is the initial temperature of the melt, $D(T_o)$ is the diffusion constant at the initial temperature, r_o is the cooling rate ($^{\circ}\text{C}/\text{hr}$) and E is the activation energy. Since the relict spinels in E40 are possibly present in two distinct size groups, we calculate cooling rates considering two limiting sizes of spinels $10\mu\text{m}$ and $60\mu\text{m}$. The calculated cooling rates range from $70^{\circ}\text{C}/\text{hr}$ to $2^{\circ}\text{C}/\text{hr}$ for an initial melt temperature of 1400°C , and from $370^{\circ}\text{C}/\text{hr}$ to $10^{\circ}\text{C}/\text{hr}$ for an initial melt temperature of 1500°C . These values are in fact lower limits as they are based on the time required for complete isotopic homogenization. Although the lower bounds of the cooling rates overlap with the cooling rates deduced from textural and mineralogical studies of CAIs (Wark and Lovering, 1982; MacPherson et al., 1984; Stolper and Paque, 1986), the upper bounds are probably closer to the true cooling rates as the higher rates are compatible with the lack of a detectable spatial gradient of $F(\text{Mg})$ in the larger spinel grains. A recent study of trace element distributions in melilite from type B1 CAIs (Davis et al., 1992) also suggests that the true cooling rates of CAIs are probably closer to the upper bound set by petrographic and textural studies ($\gg 2^{\circ}\text{C}/\text{hr}$).

The implications of the cooling rates of the parent melts of CAIs on their formation environment in the nebula was considered in detail by MacPherson et al. (1984). They noted that the cooling rate deduced from petrographic observation ($< 50^{\circ}\text{C}/\text{hr}$) are orders of magnitude higher than the cooling rate for the solar nebula as a whole ($10^{-5}\text{K}/\text{hr}$), but, are much lower than that for a radiating droplet in a low density solar nebula ($\sim 10^5\text{C}/\text{hr}$). Theoretical estimate of cooling rate of a liquid droplet in a low density solar nebula ($P \leq 10^{-3}$) (Tschuyama et al., 1980 and Macpherson et al., 1984) can be made by the equation:

primitive meteorites could have formed in localized hot-spots relaxes the requirement of an uniformly hot solar nebula, with initial temperature exceeding the melting/condensation temperatures of the refractory phases, in the region of their formation. A low temperature nebula will also be in conformity with standard models for the solar nebula (e.g., Wood and Morfill, 1988). The presence of localized hot and dense microenvironments in the nebula is a pointer towards efficient gas-dust fractionation needed to explain the relatively oxidizing environment in which refractory objects like CAIs and POIs and perhaps chondrules have formed (Anders, 1985). The localized heat source cannot be identified unambiguously even though several possibilities have been suggested; these include lightening (Whipple 1966, Cameron 1966), intense flares from the protosun (Herbig 1978) and probably frictional heating due to gas drag (Wood 1983, 1984).

5.3 Mg-Al Isotopic Systematics and Isotopic Heterogeneity in the Nebula

The presence of the short-lived nuclide ^{26}Al in early solar system objects (CAIs) has been demonstrated conclusively by many workers (Lee et al. 1976, and references in Wasserburg 1985, MacPherson et al., 1988). Studies in different types of CAIs from carbonaceous meteorites belonging to CV and CO groups and individual refractory grains like corundum and hibonite from CM meteorites (Fahey et al. 1987a, Ireland et al. 1990, Virag et al. 1991) have been carried out to obtain information on the initial distribution of ^{26}Al in the solar nebula at the time of formation of these refractory phases. The importance of studying this aspect arises from the following reasons:

- (i) if the distribution of ^{26}Al in the nebula is homogeneous it may be used as a chronometer for early solar system processes.
- (ii) ^{26}Al is a potential heat source for melting and differentiation of meteorite parent bodies.

$$\frac{dT}{dt} = \frac{3\epsilon\sigma}{r\rho \left(C_P + \frac{\Delta H_c}{\Delta T_c} \right)} [T^4 - T_o^4] \quad (5.3)$$

where T and T_o are the absolute temperatures of the liquid and surrounding medium, ϵ is the emissivity, taken to be 0.8 (Carslaw and Jaeger, 1959), σ is the Stefan-Boltzman constant ($5.7 \times 10^{-12} \text{Jcm}^{-2}\text{sec}^{-1}\text{K}^{-4}$), ρ is the density which is $\sim 2.8 \text{gm/cm}^3$ (Bottinga and Weill, 1970), r is the radius ($\sim 0.25 \text{cm}$), C_P is the specific heat ($\sim 1.5 \text{J/gm}^\circ\text{K}^{-1}$; Carmichael et al., 1977), ΔH_c is the latent heat of crystallization ($\sim 550 \text{J/gm}$), and ΔT_c is the temperature interval over which the liquid crystallizes ($\sim 350^\circ\text{K}$; MacPherson et al. 1984). Since we have considered 1400°C (1673°K) and 1500°C (1773°K) as the initial melt temperature of type B1 CAIs like E40, we calculate the cooling rates when the ambient gas temperature T_o is comparable to these two temperatures. When the initial melt temperature is 1773°K and T_o is equal to 1772°K and 1763°K the cooling rates are $\sim 515^\circ\text{C/hr}$ and 5070°C/hr respectively. Similarly when initial melt temperature is 1673°K and when T_o is equal to 1672°K and 1663°K the cooling rates are $\sim 428^\circ\text{C/hr}$ and $\sim 4250^\circ\text{C/hr}$. These calculations show that if the ambient temperature of the nebula is only 1°K less than the liquid droplet the theoretically estimated cooling rates are comparable to the upper limits obtained by our isotopic data. However theoretical models of solar system formation predict temperatures of $< 1000^\circ\text{K}$ in the region of meteorite formation (Wood and Morfill 1988). Even though some theoretical estimate of higher nebular temperature has been made (Boss, 1993), they are still much below the required value of $>1600^\circ\text{K}$. Thus a low pressure, low temperature environment cannot satisfy the constraint on cooling rates deduced from the observed data in CAIs. One is therefore constrained to invoke localized hot and dense regions in the nebula that will allow for both partial melting of solids and cooling rates appropriate for the formation of CAIs. Sheng et al. (1991a) have made such a suggestion for the formation of most of the refractory objects in the early history of the solar system, by extending their arguments based on the observation of relict spinels in plagioclase-olivine-inclusions (POIs), a class of less refractory objects from carbonaceous chondrites that have probably formed at a later time than the CAIs. The possibility that the refractory objects/phases found in

If the distribution of ^{26}Al is homogeneous it can also be used to pinpoint the astrophysical site(s) which could have contributed ^{26}Al to the solar nebula. In this section we discuss the Mg-Al isotopic data for the Efremovka and Grosnaja CAIs to address the above questions. The presence of excess ^{26}Mg in refractory phases resulting from *in situ* decay of ^{26}Al should satisfy the following relation between measured $^{26}\text{Mg}/^{24}\text{Mg}$ in the phases and the initial value of ($^{26}\text{Al}/^{27}\text{Al}$) at the time of their formation:

$$\left(\frac{^{26}\text{Mg}}{^{24}\text{Mg}}\right)_m = \left(\frac{^{26}\text{Mg}}{^{24}\text{Mg}}\right)_i + \left(\frac{^{26}\text{Al}}{^{27}\text{Al}}\right)_i \left(\frac{^{27}\text{Al}}{^{24}\text{Mg}}\right)_m \quad (5.4)$$

The CAIs from Efremovka show well behaved Mg-Al systematics (Fig.4.1) except in E44 where one can see discordance in Mg-Al isotopic data for two different mineral phases [melilite and anorthite] (Fig.4.1d). A minor disturbance can be discerned in the anorthite data for the inclusion E60 (Fig.4.1g) where individual anorthite data yield a range of initial $^{26}\text{Al}/^{27}\text{Al}$ values. Amongst the Grosnaja CAIs only GR2 (Fig.4.1i) has a well behaved systematics but with much lower initial ($^{26}\text{Al}/^{27}\text{Al}$) than the Efremovka CAIs. *The presence of ^{26}Mg excess and its correlation with ($^{27}\text{Al}/^{24}\text{Mg}$) in most of the Efremovka CAIs and in the Grosnaja CAI GR2 confirm the presence of live ^{26}Al in the region of solar nebula where these CAIs formed.*

An important observation that can be made from our data is the fact that the initial ($^{26}\text{Al}/^{27}\text{Al}$) in all but one of the Efremovka inclusions is close to the canonical value of 5×10^{-5} (Fig. 5.6) seen primarily in unaltered type B1 CAIs from CV and CO chondrites [MacPherson et al 1988 and Clayton et al. 1988 and references therein]. The Efremovka CAIs analyzed by us represent four major petrographic types (A, B1, B2, and hibonite rich) and none of them have any distinct signatures of major secondary petrographic alteration. On the other hand, all the Grosnaja CAIs representing three petrographic types [A, B and C (anorthite rich)] have distinct signatures of secondary petrographic alteration [presence of calcite, garnet, Na-rich plagioclase etc] and are characterized by disturbed Mg-Al systematics and/or much lower initial $^{26}\text{Al}/^{27}\text{Al}$ values (0 to 6×10^{-6}). A similar

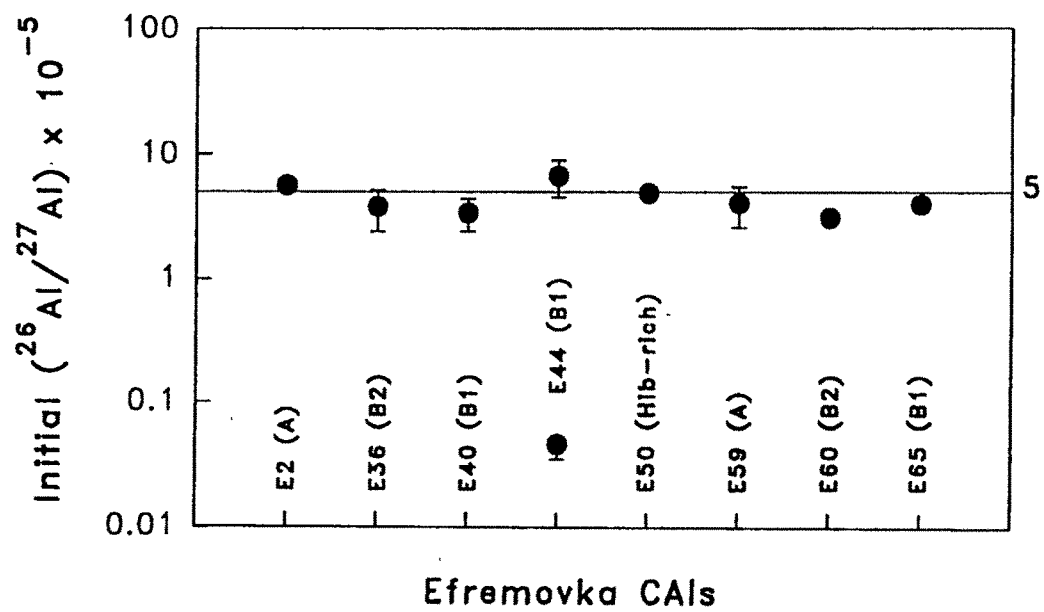


Figure 5.6: Initial $^{26}\text{Al}/^{27}\text{Al}$ in eight Efremovka CAIs analyzed for their magnesium isotopic systematics. The analyzed CAIs represent four petrographic types (A, B1, B2 and hibonite-rich).

situation holds for CAIs studied in earlier work (Macpherson et al., 1988 and references therein) with initial ($^{26}\text{Al}/^{27}\text{Al}$) varying over a wide range from 0 to 5×10^{-5} . Till date more than 500 inclusions and/or refractory phases have been analyzed from carbonaceous chondrites for their Mg isotopic composition and the main observations are :

- (i) a good number of type B1 inclusions show well behaved Mg-Al isochron with initial ($^{26}\text{Al}/^{27}\text{Al}$) close to 5×10^{-5} often referred to as the canonical value,
- (ii) in general type B2 and type A inclusions either have disturbed Mg-Al systematics or have much lower initial ($^{26}\text{Al}/^{27}\text{Al}$) ratio with few exceptions,
- (iii) hibonite-rich inclusions from CM meteorites that have large Ti and Ca isotopic anomalies have initial ($^{26}\text{Al}/^{27}\text{Al}$) that are one or two orders of magnitude lower than the canonical value, and more often devoid of excess ^{26}Mg ; on the other hand hibonites with initial Al isotopic composition close to the canonical value do not show large Ti and Ca isotopic anomaly,
- (iv) Corundum grains fall into distinct groups with different initial Al isotopic composition, the highest being close to the canonical value.

The observed variation in initial $^{26}\text{Al}/^{27}\text{Al}$ ratio in CAIs and refractory phases in different meteorites may be attributed to one or more of the following:

- (i) differences in the time of formation of CAIs and the refractory phases (assuming a uniform distribution of ^{26}Al in the nebula)
- (ii) heterogeneous distribution of ^{26}Al in the solar nebula
- (iii) secondary alteration of some of the objects leading to disturbances in the Mg-Al isotopic systematics.

If the variations are simply ascribed to time assuming a uniform distribution of ^{26}Al in the solar nebula with initial $^{26}\text{Al}/^{27}\text{Al}$ close to the canonical value it would imply a

large time interval ($> 5\text{Ma}$) between the formation of type B1 inclusions and other types of inclusions and some of the refractory phases in CM meteorites. This is a difficult proposition as hibonites found in CM chondrite are more refractory than the phases seen in type B1 CAIs, and they also have much larger Ti/Ca isotopic anomalies than in the case of type B1 CAIs and were either contemporaneous or formed prior to the CAIs. These considerations have led many researchers to propose extreme heterogeneity in the distribution of ^{26}Al in the solar nebula as the cause for the observed variation in the initial $^{26}\text{Al}/^{27}\text{Al}$ seen in refractory phases and CAIs from carbonaceous chondrites. Even though, the fact that bulk of the CAIs analyzed to date have signatures of secondary alteration in low temperature environment which can potentially disturb the Mg-Al systematics leading to low or near absence of ^{26}Al in these objects was noted, it was not emphasized to be the main cause for the observed variations.

The most important feature of the results obtained from this study suggest that the canonical value of 5×10^{-5} for the initial ($^{26}\text{Al}/^{27}\text{Al}$) ratio is not restricted to type B1 CAIs alone. This allows us to generalize upon our results. On the basis of Efremovka data one can question the validity of extreme spatial heterogeneity in the distribution of ^{26}Al in the solar nebula in the region of formation of Efremovka CAIs. Data obtained in this study suggest that all the Efremovka CAIs have most probably sampled the same ^{26}Al reservoir and the variation seen in E60 and E44 may be attributed to secondary processes. In fact the presence of nepheline in E60 indicates possible presence of secondary processes affecting the anorthites. The initial Mg isotopic ratio in E60 which is 2‰ above the reference value is also suggestive of secondary event leading to reequilibration of Mg isotopic systematics in the CAI. The discordant data for melilite and anorthite in E44 is exactly what one expects if there was an exchange of Mg between these two phases with contrasting Al/Mg ratios. Podošek et al., (1991) proposed such a scenario to explain the observed Mg-Al systematics in several Allende CAIs that have disturbed record of secondary alteration, and suggested that secondary processes leading to exchange/reequilibration of Mg isotopes is the main cause for the observed disturbances in Mg-Al systematics seen in petrographically altered CAIs. The Efremovka data, therefore, do not support the idea of an extreme spatial

inhomogeneity of ^{26}Al in the solar nebula. However, we cannot rule out the possibility that there can be more than one distinct reservoir of ^{26}Al in the nebula, particularly in light of the data for hibonite and corundum from CM meteorites. Virag et al., (1991) have in fact suggested the presence of three distinct ^{26}Al reservoir, two of them with initial ($^{26}\text{Al}/^{27}\text{Al}$) $\sim 5 \times 10^{-5}$ and $\sim 2 \times 10^{-6}$ and a third one without ^{26}Al to explain the Mg-Al isotopic systematics in Murchison corundum grains. Although, these grains may have probably sampled a restricted area of the solar nebula, this observation coupled with Efremovka data suggest probable presence of specific zones/reservoirs in the nebula with distinct ($^{26}\text{Al}/^{27}\text{Al}$) isotopic composition.

In the light of isotopic homogeneity of ^{26}Al proposed above for the region in the nebula where the Efremovka CAIs have formed, we shall consider the spatial extent of such homogeneity in comparison to the nebular distribution of ^{16}O and ^{50}Ti , two stable isotopes with anomalous (enriched) abundances in many refractory phases. Oxygen is one of the major elements in the solar system. Isotopic composition of O has been studied extensively in CAIs, chondrules, meteorites, and lunar and terrestrial samples (Clayton 1978, 1993 and references therein). Oxygen has three isotopes (16, 17 and 18) and isotopic ratios are normalized with respect to ^{16}O which is the most abundant isotope, and the isotopic data of oxygen is expressed as deviation ($\delta^{17}\text{O}$ and $\delta^{18}\text{O}$) from the reference value (standard mean ocean water). On the three isotope plot of $\delta^{17}\text{O}$ vs $\delta^{18}\text{O}$ the oxygen isotopic data from different samples are expected to lie on a fractionation line with slope equal to half. However, oxygen isotopic data for refractory phases in CAIs fall on a line with slope ~ 1 (Clayton et al., 1973; Clayton 1978, 1993 and references therein). The individual phases in CAIs show a great variation in oxygen isotopic composition. Certain phases like spinel show a maximum enrichment in ^{16}O ($\delta^{17}\text{O} \sim -40\%$) and phases like melilite have almost normal isotopic composition. The internal variations have been interpreted as having originated from secondary exchange of O with an external gaseous reservoir. The most ^{16}O rich mineral exchanged the least with this external reservoir whereas the least ^{16}O rich phase experienced maximum exchange, probably due to greater diffusion rates of oxygen (Muehlenbachs and Kushiro 1974 and Hayashi and Muehlenbachs 1984). The

oxygen isotopic data in CAIs can be attributed to the presence of two reservoirs, one (dust) enriched in ^{16}O and another (gas) depleted in ^{16}O and the mixing of these two reservoirs generated the line with slope ~ 1 (Clayton et al. 1985). If one considers the oxygen isotopic data for bulk meteorites and terrestrial and lunar samples they fall on different lines with slope half. The fact that for large (\gg km) objects the oxygen isotopic data do not fall on a single fractionation line indicates a planetary scale heterogeneity in oxygen. On the other hand Ti isotopic anomalies particularly enrichment and at times depletion in the neutron rich isotopes (^{49}Ti and ^{50}Ti) seen in hibonite grains from CM meteorites, show a random scatter in their absolute magnitude. Fahey et al., (1985, 1987a) and Zinner et al., (1986b), suggested that these random variations arise from plausible heterogeneous distribution of the carriers of these anomalies viz. interstellar dust grains in the nebula at a very small scale length. It is interesting to note that Ti-rich phases like pyroxene in type B1 CAIs from CV meteorites have nearly normal Ti isotopic composition. Thus it seems that Ti isotopic variations occur at a spatial scale length that is much smaller than that of ^{26}Al which in turn is perhaps smaller than planetary scale length in the variation of oxygen isotopic distribution in the nebula.

5.4 ^{41}Ca In The Early Solar System

The studies of potassium isotopic composition in Efremovka CAIs, results of which were presented in the previous chapter (Table 4.6) was intended to look for the presence of the short-lived radionuclide ^{41}Ca ($\tau \sim 0.15\text{Ma}$) in the early solar system. The unaltered Efremovka CAIs with initial ($^{26}\text{Al}/^{27}\text{Al}$) close to the canonical value of 5×10^{-5} and containing phases like pyroxene and perovskite with high Ca/K are ideal to look for possible presence of ^{41}Ca in the solar nebula at the time of formation of these CAIs. Previous attempts in this direction (Stegmann and Specht 1983, Hutcheon et al. 1984) using CAIs from Allende and Leoville were not very successful although the data of Hutcheon et al., (1984) provided a hint for the presence of ^{41}Ca in a couple of Allende CAIs with an upper limit of $(8 \pm 3) \times 10^{-9}$ for the initial ($^{41}\text{Ca}/^{40}\text{Ca}$) at the time of their formation. If

^{41}K excess resulting from ^{41}Ca decay is present in refractory phases of CAI one can write the following relation for K-Ca systematics:

$$\left(\frac{^{41}\text{K}}{^{39}\text{K}}\right)_m = \left(\frac{^{41}\text{K}}{^{39}\text{K}}\right)_t + \left(\frac{^{41}\text{Ca}}{^{40}\text{Ca}}\right)_t \left(\frac{^{40}\text{Ca}}{^{39}\text{K}}\right)_m \quad (5.5)$$

The results obtained in the present study, shown in Fig. 5.7, clearly demonstrates that presence of excess ^{41}K in the analyzed phases, particularly those with $\text{Ca}/\text{K} > 3 \times 10^5$. A very good correlation between ^{41}K and the ^{40}Ca content of the analyzed phases has also been observed. The best fit line through the data points yields an initial $(^{41}\text{K}/^{39}\text{K})$ close to the reference value of 0.072 and has a slope of $(1.6 \pm 0.3) \times 10^{-8}$. Even though the Ca/K value for most of the data points lie in the region of $(0.3 \text{ to } 3) \times 10^6$, the correlation holds true even for phases with extreme Ca/K ratio of 2×10^7 . The value of the slope of the correlation line obtained by us is higher than the value $[8 \pm 3] \times 10^{-9}$ reported by Hutcheon et al. (1984). However, a majority of the data points (4 out of 6) with high $^{40}\text{Ca}/^{39}\text{K}$ ($> 5 \times 10^5$) reported by Hutcheon et al. (1984) suggest a higher value for the slope that is closer to the value obtained by us.

We, therefore, believe that the excess ^{41}K signal seen by us in the Efremovka CAIs are real and consider the possible causes for this excess. The observed ^{41}K excess in the Efremovka CAIs can result from any one of the following reasons:

- (i) production of ^{41}Ca by secondary neutrons during cosmic ray exposure of the Efremovka meteorite resulting from (n, γ) reaction with ^{40}Ca present in the CAIs and its subsequent decay,
- (ii) ^{41}K locked in refractory stardust that are part of the initial components of the solar nebula from which the CAIs are formed,
- (iii) presence of the short-lived radionuclide ^{41}Ca in the early solar system that was incorporated 'live' into the CAIs during their formation and its *in situ* decay.

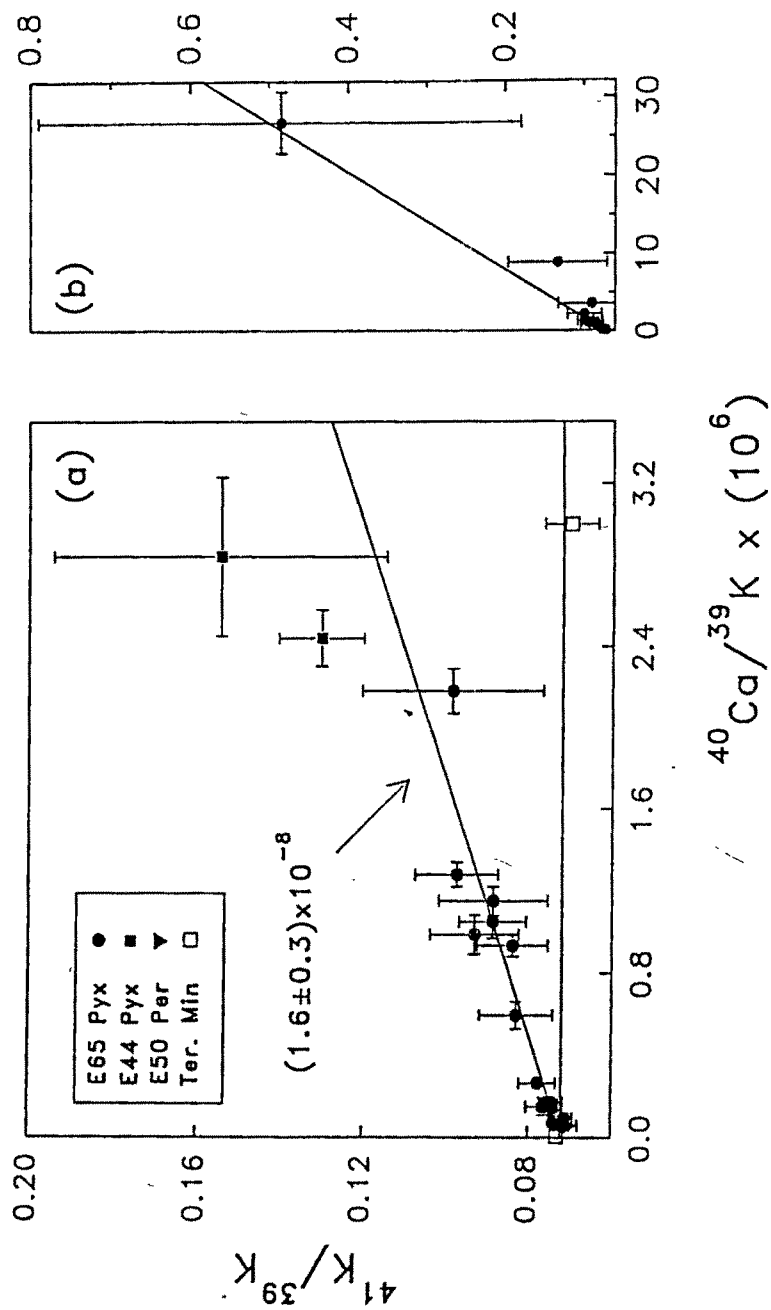


Figure 5.7: Plot of measured potassium isotope ratios as a function of $^{40}\text{Ca}/^{39}\text{K}$ for refractory perovskite(Per) and pyroxene(Pyx) phases in CAIs E50, E44 and E65. For clarity, phases with $\text{Ca}/\text{K} \leq 3.5 \times 10^6$ are shown in Fig(a), while all data points are shown in Fig(b). The open symbols represent data for terrestrial pyroxene, the horizontal line represents the reference potassium isotope ratio (0.072) and the slope of the best fit line is $(1.6 \pm 0.3) \times 10^{-8}$.

As already noted an important observation in this study is the extremely good correlation of excess ^{41}K with ^{40}Ca contents of the analyzed phases. The observed correlation between excess ^{41}K and ^{40}Ca is a natural expectation if the excess ^{41}K is either due to cosmic ray induced effect or due to the presence of ^{41}Ca in the early solar system. On the other hand, such a correlation is difficult to explain in the 'fossil' hypothesis.

If the excess ^{41}K is due to cosmogenic production of ^{41}Ca , the secondary neutron fluence experienced by the Efremovka meteorite should be sufficient to account for the $^{41}\text{Ca}/^{40}\text{Ca}$ ratio of $(1.6 \pm 0.3) \times 10^{-8}$ which represents the slope of the correlation line in Fig. 5.7. With a thermal neutron cross section of 440mb for the $^{40}\text{Ca}(n,\gamma)^{41}\text{Ca}$ (Mughabghab et al., 1981) reaction, a thermal neutron fluence of $\sim 3 \times 10^{16}$ is necessary to explain the observed ratio. Although no direct estimate of the thermal neutron fluence experienced by the Efremovka samples is available a reasonable estimate can be made by comparing it with Allende, as both of them belong to the same meteorite type (CV3). The expected secondary fluence in a meteorite depends mainly on three parameters: the cosmic ray exposure duration, the pre-atmospheric size and the chemical composition of the meteorite. The preatmospheric size is an important parameter as the production of secondary neutrons within the meteorite increases with shielding depth and reaches a maximum at a shielding depth of $\sim 100\text{-}150\text{gmcm}^{-2}$. The noble gas data for the Efremovka meteorite (Mazor et al., 1970) suggest a cosmic ray exposure age of $\sim 10\text{Ma}$ for this meteorite which is twice that for the Allende (Fireman and Gobel 1970). However, the pre-atmospheric size of Efremovka, with a recovered mass of $\sim 21\text{Kg}$, is likely be much smaller than that of Allende for which the recovered mass exceeds 2000Kg. A fairly reliable estimate of the neutron fluence experienced by Allende has been made by Gobel et al., (1982) based on studies of the neutron produced isotope ^{36}Ar (from ^{36}Cl). The inferred values are a few times 10^{14}cm^{-2} (up to 10^{15}cm^{-2}). Even if we consider the higher value of neutron fluence estimated for Allende and the factor of two higher exposure age of Efremovka compared to Allende, the neutron fluence experienced by Efremovka cannot exceed a few times 10^{15}cm^{-2} in view of its smaller pre-atmospheric size. This fluence is an order of magnitude less than that required to explain the observed ^{41}K excess in the Efremovka CAIs. Therefore, the

possibility that the observed ^{41}K excess is due to production by secondary neutrons during the cosmic ray exposure of the Efremovka meteorite in the interplanetary space can be ruled out.

The possibility that 'fossil' records of extinct nuclide decay products may be found in primitive meteorite was proposed by Clayton (1977, 1982, 1986). He has also suggested specifically that ^{41}K of 'fossil' origin could be present in refractory inclusions of primitive meteorites, which would enhance the $^{41}\text{K}/^{39}\text{K}$ ratio in these objects above the normal solar system value (Clayton 1977). In this model the refractory condensates (stardust) formed in stellar environment (e.g. supernova envelope) will be enriched in their refractory element concentrations (e.g. Ca) compared to the volatile (e.g. K) and as such they will have high Ca/K ratio and also excess ^{41}K from ^{41}Ca decay. Since these stellar condensates are expected to be an important component of the solar nebula they will find their way into the CAIs that are considered to be some of the first solids to form in the solar system via processes invoking condensation, evaporation, and/or melting/recrystallization. These CAIs can therefore inherit excess ^{41}K from the stellar condensates. The magnitude of ^{41}K excess in the CAI will depend upon several parameters including the initial elemental fractionation in the stellar environment during the formation of the stellar condensates and the degree of enrichment of stellar condensates, relative to normal solar system matter, in the parent material from which the CAIs are formed. While this scenario has its own appeal, it does not readily explain the correlation between excess ^{41}K and ^{40}Ca content seen in our data. One may attempt to explain this correlation by considering mixing of two components during the formation of the CAIs with one of the components having both high (Ca/K) ratio and large ^{41}K excess and the other with lower ratio and normal potassium isotopic composition (Clayton, 1993). Such a scenario appears *ad hoc* and there are quite a few free parameters, particularly fractionation factors, whose values cannot be easily constrained. The data presented by us suggest an enrichment in the $^{41}\text{K}/^{39}\text{K}$ ratio by a factor of six in the pyroxene with the highest Ca/K value. Thus in the 'fossil' model, the stellar condensates must be characterized by values that are much higher than this enrichment factor, a proposition difficult to accommodate. It may also be noted that

Clayton (1977) predicted an enhancement of only 0.25% for the $^{41}\text{K}/^{39}\text{K}$ value in CAI based on this model. Thus it is extremely unlikely that the observed ^{41}K excess could be of 'fossil' origin. The presence of a small component of 'fossil' ^{41}K in the CAIs however cannot be ruled out unequivocally.

The ^{41}K excess in the Efremovka CAIs and its correlation with ^{40}Ca can therefore be best explained by considering the presence of live ^{41}Ca in the early solar system at the time of formation of the Efremovka CAIs. Because of the short half-life of ^{41}Ca , the observation of ^{41}K excess in early solar system objects puts some stringent constraint on the time interval between the last nucleosynthetic input to the solar nebula and the formation of some of the first solar system solids (CAIs). We shall consider these time scales based on ^{26}Al and ^{41}Ca data in Efremovka CAIs in the following section.

5.5 Extinct Radionuclides and Time Scales for Early Solar System Process

The presence of short-lived nuclei decay product in CAI allow us to constrain the time interval between the last injection of nucleosynthetic matter to the solar nebula and the formation of these objects. The strictest lower limit on this time interval is provided by the observation of radionuclide with the shortest meanlife. Prior to this study ^{26}Al ($\tau \sim 1.1\text{Ma}$) was the shortest lived radionuclide whose presence in the early solar system was conclusively established. The present study showed that ^{41}Ca with a six times shorter meanlife ($\sim 0.15\text{Ma}$) than ^{26}Al was also present in the early solar system. As a first approximation we assume that that all the solar system Al, Mg, Ca and K was injected during the last nucleosynthetic event prior to the isolation of the nebula. The time interval ' Δ ' between injection of this matter [containing ^{26}Al and ^{41}Ca] into the solar nebula and formation of CAIs is given by the relation:

$$\Delta = -\frac{1}{\lambda} \cdot \ln \left[\frac{M}{P} \right] \quad (5.6)$$

where M is the measured ratio, P is the production ratio and λ is the radioactive decay constant for the particular nuclide. Before we apply the above relation to evaluate Δ we consider the production ratios of ($^{26}\text{Al}/^{27}\text{Al}$) and ($^{41}\text{Ca}/^{40}\text{Ca}$) in the various astrophysical sites. A discussion on the plausible nucleosynthetic sites for ^{26}Al is given by Clayton and Leising (1987); these are:

- (i) explosive nucleosynthesis in supernova where $P \sim 10^{-3}$ (Truran and Cameron 1978, Woosley and Weaver 1980),
- (ii) hydrostatic carbon burning in massive stars $P \sim 10^{-3}$ (Arnett and Wefel 1978),
- (iii) high temperature hydrogen burning in nova and asymptotic giant branch stars where $P \sim 0.1$ to 1 (Hillebrandt and Theileman 1982, Cameron 1985, and Wasserburg et al. 1994).

While the production ratio of ($^{26}\text{Al}/^{27}\text{Al}$) vary over a wide range the situation in case of ^{41}K which is believed to be produced as its radioactive progenitor ^{41}Ca is simpler. The nucleosynthetic processes that have been considered for production of ^{41}Ca are:

- (i) explosive oxygen burning: $P \sim 1.5 \times 10^{-3}$ (Woosley et al. 1973),
- (ii) explosive silicon burning: $P \sim 10^{-3}$ (Bodansky et al. 1968).

The production ratio of ($^{41}\text{Ca}/^{40}\text{Ca}$) can also be estimated by considering the solar system abundance of K and Ca isotopes. Since ^{41}Ca is the radioactive progenitor of ^{41}K , the production ratio is $\sim 4 \times 10^{-3}$. If we consider equal production of the odd mass nuclides ^{41}Ca and ^{43}Ca we get a production value of 1.3×10^{-3} . The production ratio for ^{41}Ca is thus much more tightly constrained than ^{26}Al and ranges from $[1\text{ to }4] \times 10^{-3}$.

Based on the above production ratios (P) for ^{26}Al and the measured ratio (M) of 5×10^{-5} in CAIs the estimated time interval Δ varies from 3 to 10Ma. In the case of ^{41}Ca , the value for Δ is $< 1.5\text{Ma}$ for a measured ratio of 1.6×10^{-8} . If we assume that the injection of ^{26}Al

and ^{41}Ca into the solar nebula had taken place contemporaneously we can use data for both ^{26}Al and ^{41}Ca and get a value of Δ by using the relation:

$$\Delta = -\frac{1}{\lambda_i - \lambda_j} \cdot \ln \left[\frac{M_i}{P_i} \cdot \frac{P_j}{M_j} \right] \quad (5.7)$$

where P_i and P_j refer to production ratios, M_i and M_j refer to measured ratios in CAIs, and λ_i and λ_j refer to the decay constants of the two short-lived radionuclides. For the range of above mentioned production ratios for ^{26}Al and ^{41}Ca , Efremovka CAIs yield Δ value in the range of 0.6 to 2Ma.

However, these values are upper limits as the above relation does not take into account the dilution of the freshly injected matter with pre-existing nebular matter of normal composition. There is no simple way of rigorously estimating this dilution factor. One can only make an order of magnitude calculation based upon the short lived radioisotope ^{129}I ($\tau \sim 23\text{Ma}$). The production processes of iodine isotopes are well understood, and the production ratio of $^{129}\text{I}/^{127}\text{I}$ is of the order of unity. The measured initial value of $^{129}\text{I}/^{127}\text{I}$ in meteoritic phases is $\sim 10^{-4}$. If the decrease in the initial ratio from its value at production is ascribed to free decay interval ' Δ ' then the time interval is ~ 200 Ma. However, the presence of ^{26}Al and ^{41}Ca in CAIs show that free decay interval is only a few million years, which is negligible compared to the meanlife of ^{129}I . Therefore, one can postulate a dilution factor of $\sim 10^4$ to explain the measured initial $^{129}\text{I}/^{127}\text{I}$ ratio. One must however note that ^{129}I has a meanlife much greater than that of ^{26}Al and ^{41}Ca and therefore, it could have been produced over a much longer time scale in different stellar sites/sources and these individual contributions cannot be easily decoupled. Further, there is no *a priori* way of predicting whether all short-lived nuclei were introduced into the solar nebula from the same source(s) and got diluted to the same extent. Wasserburg et al., (1994) have recently proposed a similar dilution factor by considering data for various short-lived nuclides in the early solar system and assuming a common source (AGB star) for their origin. A nebular dilution factor of $\sim 10^4$ combined with the measured and production ratios of ^{41}Ca

in Efremovka CAIs yield a time interval Δ of $< 1\text{Ma}$. Even though the uncertainty in the proper choice of $^{26}\text{Al}/^{27}\text{Al}$ makes it difficult to exactly obtain this time scale, the required production rate that will yield a time scale compatible with that obtained from ^{41}Ca is 0.15 which is within the range predicted for different stellar sites. The ^{41}Ca data predicts the strictest lower limit for the time interval between the injection of freshly synthesized nucleosynthetic matter to the solar nebula and formation of CAIs. The time scale obtained from ^{41}Ca is also consistent with the recent observation of ^{60}Fe in differentiated meteorites (Shukolyukov and Lugmair 1993a, b) which suggest that the time interval between the isolation of the nebula and the formation of large ($\gg \text{km}$ -sized) objects and their subsequent heating, melting and recrystallization is $< 10\text{Ma}$.